Bioorganic Chemistry 88 (2019) 102952

Contents lists available at ScienceDirect

Bioorganic Chemistry

journal homepage: www.elsevier.com/locate/bioorg

Design, synthesis and molecular docking of new *N*-4-piperazinyl ciprofloxacin-triazole hybrids with potential antimicrobial activity

Hamada H.H. Mohammed[a,b], El-Shimaa M.N. Abdelhafez[a], Samar H. Abbas[a], Gamal A.I. Moustafa[a], Glenn Hauk[c], James M. Berger[c], Satoshi Mitarai[d], Masayoshi Arai[e], Rehab M. Abd El-Baky[f], Gamal El-Din A. Abuo-Rahma[a,*]

[a] Department of Medicinal Chemistry, Faculty of Pharmacy, Minia University, Minia 61519, Egypt
[b] Department of Pharmaceutical Chemistry, Faculty of Pharmacy, Deraya University, New-Minia 61519, Egypt
[c] Deprtment of Biophysics and Biophysical Chemistry, Johns Hopkins University School of Medicine, Baltimore, MD, USA
[d] Bacteriology Division, Department of Mycobacterium Reference and Research, Research Institute of Tuberculosis, Japan Anti-Tuberculosis Association, Kiyose 204-8533, Japan
[e] Graduate School of Pharmaceutical Sciences, Osaka University, 1-6 Yamadaoka, Suita, Osaka 565-0871, Japan
[f] Department of Microbiology & Immunology, Faculty of Pharmacy, Minia University, Minia 61519, Egypt

ARTICLE INFO

Keywords:
Ciprofloxacin
Antimycobacterial
Antibacterial
Antifungal
DNA cleavage assay
Molecular docking

ABSTRACT

New *N*-4-piperazinyl ciprofloxacin-triazole hybrids **6a-o** were prepared and characterized. The *in vitro* antimycobacterial activity revealed that compound **6a** experienced promising antimycobacterial activity against *Mycobactrium smegmatis* compared with the reference isoniazide (INH). Additionally, compound **6a** exhibited broad spectrum antibacterial activity against all the tested strains either Gram-positive or Gram-negative bacteria compared with the reference ciprofloxacin. Also, compounds **6g** and **6i** displayed considerable antifungal activity compared with the reference ketoconazole. DNA cleavage assay of the highly active compounds **6c** and **6h** showed a good correlation between the *Mycobactrium* cleaved DNA gyrase assay and their *in vitro* antimycobactrial activity. Moreover, molecular modeling studies were done for the designed ciprofloxacin derivatives to predict their binding modes towards Topoisomerase II enzyme (PDB: 5bs8).

1. Introduction

Fluoroquinolones are considered one of the most widely prescribed antimicrobial agents for treatment of bacterial infections. In addition to their broad antibacterial spectrum, fluoroquinolones are well tolerated with excellent safety profile and favorable pharmacokinetic properties [1–3].The antibacterial activity of fluoroquinolones is achieved through the inhibition of type II bacterial topoisomerase enzymes, DNA gyrase (subunits encoded by gyrA and gyrB), an enzyme involved in DNA replication, recombination and repair. They can also bind to topoisomerase IV (subunits encoded by par C and par E). Cell death is caused by trapping topoisomerase protein–DNA complex in order to disrupt normal DNA replication, inducing DNA damage, and triggering cell death mechanisms [4–6]. Furthermore, many research studies showed other biological activities for fluoroquinolones such as antifungal [7,8], antitubercular [9,10], antitumor [11–13], Urease inhibitory activity [14], anti-HIV-1 integrase and anti-HCV-NS3 helicase [15]. Fluoroquinolones like ciprofloxacin, ofloxacin and levofloxacin were approved by WHO as second line agents for the treatment of tuberculosis (TB) mainly in cases involving resistance to first-line anti-TB drugs [16]. DNA gyrase is considered to be the main drug target of fluoroquinolones in *Mycobacterium tuberculosis* [17]. However, increasing bacterial resistance to ciprofloxacin due to some extent of misuse has put enormous pressure on the researchers all over the world to find newer derivatives of fluoroquinolones to combat such resistance.

According to structure activity relationship (SAR) of fluoroquinolones, the side chain substitution at C-7 position is so essential where it affects the physicochemical properties, bioavailability, lipophilicity and safety of fluoroquinolones [12,18–24]. Mycobacteria have lipid rich cell wall, and lipophilicity is an important consideration in the design of newer antitubercular agents [25]. Current research on fluoroquinolones revealed that increasing the lipophilicity at C-7 was found to have more potent antibacterial or antimycobaterial activity than the corresponding parent fluoroquinolones [26]. Furthermore, introduction of triazole moiety into *N*-1 position of fluoroquinolones was found to have a great potential to compete the drug-resistant

* Corresponding author.
E-mail address: gamal.aborahma@mu.edu.eg (G.E.-D.A. Abuo-Rahma).

https://doi.org/10.1016/j.bioorg.2019.102952
Received 19 August 2018; Received in revised form 20 April 2019; Accepted 24 April 2019
Available online 25 April 2019

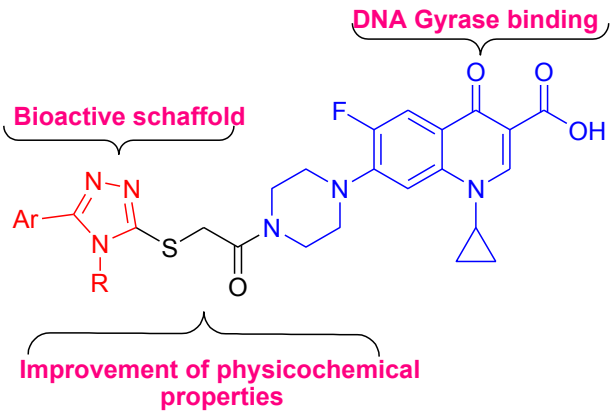

Fig. 1. Design of the target compounds.

bacterial infections. Moreover, previous research studies indicated that incorporation of a triazolyl ethanol moiety in the C-7 side chain of ciprofloxacin showed a marked growth inhibition of all the tested strains of bacteria and fungi. A research study illustrated that incorporation of the antibacterial quinolones with the triazole moiety couldn't only enhance the antimicrobial activities, but also remarkably broaden the antimicrobial spectrum [27]. Meanwhile, combination of fluoroquinolones with other antibiotics or known bioactive entities is one measure to introduce potent antimicrobial molecules effective against resistant and anaerobic bacterial strains [28].

Due to the promising perspective of fluoroquinolones in treatment of TB, as well as the urgent need of newer analogues in order to overcome the problem of bacterial resistance, the aim of this work is to synthesize new *N*-4-piperazinyl ciprofloxacin-triazole hybrids (Fig. 1) with different substituents on the triazole moiety and to evaluate their antimycobacterial, antibacterial and antifungal activities. Moreover, molecular docking studies and DNA cleavage assay have been carried out to investigate the binding modes and mechanism of action of the target compounds.

2. Results and discussion

2.1. Chemistry

The target compounds **6a–o** were synthesized as outlined in Scheme 1. 5-Aryl-4*H*-1,2,4-triazole-3-thione intermediates **4a–o** were prepared as reported [29]. Acylation of ciprofloxacin with bromoacetyl bromide using K_2CO_3 as a base afforded the intermediate acylated ciprofloxacin **5** [30]. Coupling of 1,2,4-triazole-3-thione derivatives **4a–o** with acylated ciprofloxacin **5** was achieved in acetonitrile in the presence of TEA as a base to afford the target compounds **6a-o** using a reported procedure [31,32]. The newly synthesized compounds **6a-o** were identified by IR, ^{1}H NMR, ^{13}C NMR and HRMS spectral techniques. The ^{1}H NMR spectra for compounds **6a-o** showed the known characteristic pattern for the parent ciprofloxacin in addition to a singlet at δ 4.36–4.67 ppm related to (S−C$\underline{H_2}$−CO) of the linker. Also, ^{13}C NMR spectra revealed a signal at δ 166.72–166.25 ppm related to carbonyl of the (S−CH_2−$\underline{CO}$) linker. IR spectrum shows intense strong sharp peak at 1680–1690 cm^{-1} corresponding to C=O of the (S−CH_2−$\underline{CO}$) linker. HRMS (ESI) data for compounds **6a-o** confirmed their assigned structures.

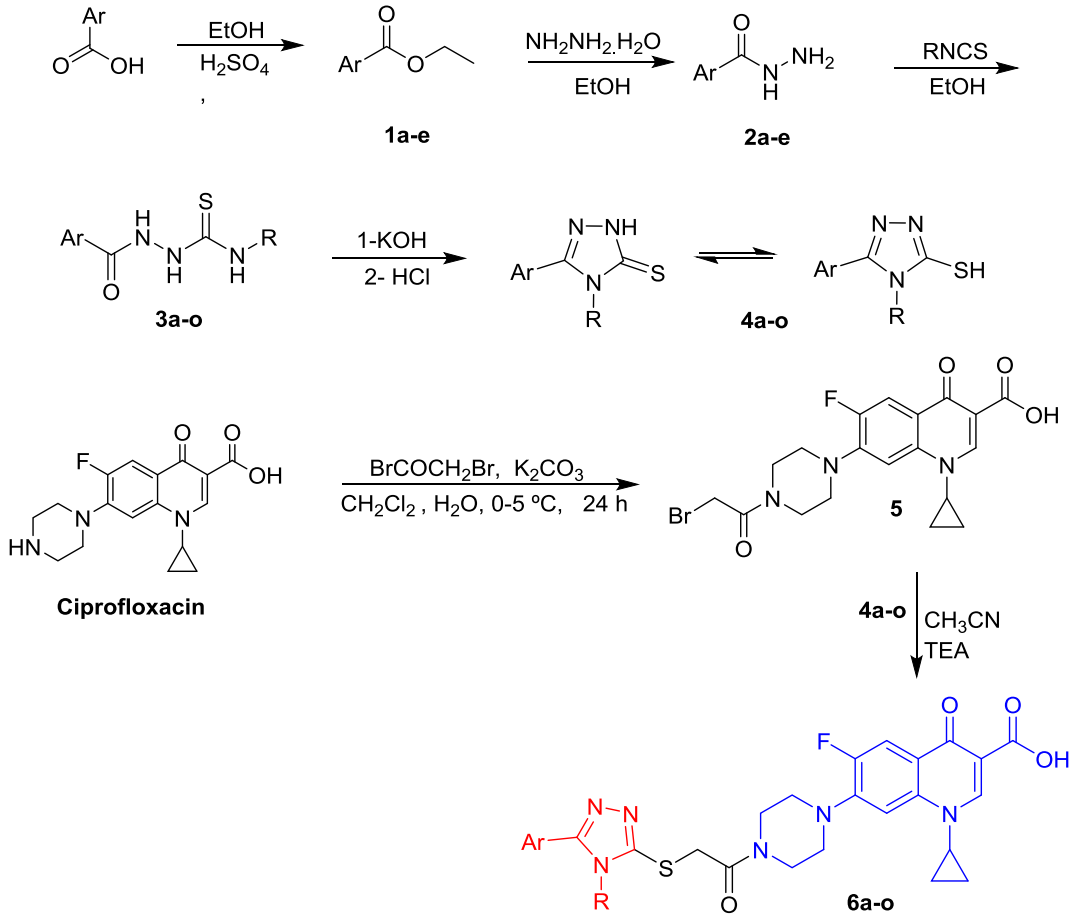

Scheme 1. Synthesis of the target compounds 6a–o.

compound	R	Ar	compound	R	Ar
1a, 2a	—	C_6H_5	**3f, 4f, 6f**	Et	C_6H_5
1b, 2b	—	4-Cl-C_6H_4	**3g, 4g, 6g**	Et	4-Cl-C_6H_4
1c, 2c	—	4-OCH_3-C_6H_4	**3h, 4h, 6h**	Et	4-OCH_3-C_6H_4
1d, 2d	—	3,4-di-OCH_3-C_6H_3	**3i, 4i, 6i**	Et	3,4-di-OCH_3-C_6H_3
1e, 2e	—	3,4,5-tri-OCH_3-$C6H_2$	**3j, 4j, 6j**	Et	3,4,5-tri-OCH_3-$C6H_2$
3a, 4a, 6a	Allyl	C_6H_5	**3k, 4k, 6k**	Ph	C_6H_5
3b, 4b, 6b	Allyl	4-Cl-C_6H_4	**3l, 4l, 6l**	Ph	4-Cl-C_6H_4
3c, 4c, 6c	Allyl	4-OCH_3-C_6H_4	**3m, 4m, 6m**	Ph	4-OCH_3-C_6H_4
3d, 4d, 6d	Allyl	3,4-di-OCH_3-C_6H_3	**3n, 4n, 6n**	Ph	3,4-di-OCH_3-C_6H_3
3e, 4e, 6e	Allyl	3,4,5-tri-OCH_3-$C6H_2$	**3o, 4o, 6o**	Ph	3,4,5-tri-OCH_3-$C6H_2$

2.2. Biological investigations

2.2.1. Screening of antimycobactrial activity

The *in vitro* antimycobacterial activity of compounds **6a-l,** and **6n-o** was initially evaluated against the non-pathogenic *M. smegmatis* using MTT assay method [33] under aerobic conditions using isonicotinic acid hydrazide (INH) as a reference. The obtained MICs (μg/mL) of the target compounds against *M. smegmatis* are outlined in Table 1.

From the results in Table 1, it is clear that the triazole derivative **6a** displayed potent antimycobacterial activity with MIC of 3.25 μg/mL compared to the reference INH. In addition, both compounds **6c** and **6 h** showed a comparable activity to that of the reference INH with MIC of 6.25 μg/mL. Compounds **6b, 6f** and **6n** exhibited lower activity with MIC of 6.25 μg/mL. Furthermore, the triazole derivatives **6e, 6g, 6i, 6j, 6k, 6l, 6n and 6n** showed very weak activity compared with the reference INH. In this study, the higher activity of compounds **6a, 6c** and **6h** clearly indicates that the *N*-allyl derivatives are more potent than the *N*-ethyl derivatives which, in turn, are more active than the *N*-phenyl derivatives. Moreover, the best aryl substituent is the *p*-OCH_3 seen in compounds **6c** and **6h**. The *N*-allyl derivative **6a** with unsubstituted phenyl moiety displayed the highest antimycobacterial activity against *Mycobacterium smegmatis*. Motivated by these results, we next evaluated the inhibitory activity of compounds **6a-c, 6f, 6h-j, 6n** and **6o** towards pathogenic drug-resistant and drug-susceptible strains of *M. tuberculosis* **(**Table 2**).**

Table 1
The MICs of the tested compounds and their reference INH against *M. smegmatis* (μg/mL).

Compound #	MIC against *M. smegmatis* (μg/mL)	Compound #	MIC against *M. smegmatis* (μg/mL)
6a	3.25	6i	100
6b	25	6j	200
6c	6.25	6k	100
6d	ND	6l	> 200
6e	200	6m	ND
6f	25	6n	25
6g	> 200	6o	200
6h	6.25	INH	5

ND: not determined.

Table 3
The MICs of antibacterial and antifungal activities of the tested compounds **6a-6b, 6e-g, 6i, 6k-6l** and **6o**, ciprofloxacin and ketoconazole (μg/mL).

#	MIC(μg/mL)				
	S.aureus	*E. coli*	*Klebsiella pneumoniae*	*Pseudomonas aeruginosa*	*Candida albicans*
6a	1.90	2.60	1.70	15.09	NA
6b	4.50	1.59	24.29	41.16	NA
6e	14.8	23.20	33.2	10.40	NA
6f	11.40	19.09	1.87	33.34	10.57
6g	13.40	9.85	12.80	67.90	3.80
6i	9.40	1.95	2.98	29.85	NA
6k	180.70	615.30	6.98	722.20	NA
6l	NA	1.47	1.42	NA	6.13
6o	1.70	6.98	71.09	1.04	NA
Ciprofloxacin	2.12	3.50	1.9	2.82	–
Ketoconazole	–	–	–	–	2.60

NA: no activity, –: Not determined.

The results in Table 2 revealed that the target compounds **6a**, **6b**, **6c**, **6f**, **6h**, **6i**, **6n** and **6o** have potential activity against the pathogenic drug-resistant and drug-susceptible strains of *M. tuberculosis* (MICs: 4–32 μg/mL). However, they are generally less active than the reference drugs LVFX and MFLX (MICs:0.03–8 μg/mL). Among them, compounds **6a** and **6h** displayed the highest activity (MICs: 4 μg/mL) against the drug resistant strain R-2012–59 (MDR). Similarly, ciprofloxacin derivatives **6b**, **6c** and **6f** exhibited activity against R-2012–59 (MDR) strain (MIC: 8 μg/mL). Also, the triazole derivatives **6a** and **6h** showed activity against H37Rv ATCC27294 strain (MIC: 8 μg/mL). Compounds **6c** and **6o** showed lower activity against R-2012-97 (XDR) strain (MIC: 16 μg/mL).

2.2.2. Screening of antibacterial and antifungal activities

The antibacterial and antifungal activities of **6a-6b, 6e-g, 6i, 6k-6l and 6o** were evaluated *in vitro* against Gram-positive bacteria *Staphylococcus aureus* (ATCC 6538), and Gram-negative bacteria such as *Klebsiella pneumoniae* (ATCC 10031), *Pseudomonas aeruginosa* (ATCC 10145), Escherichia coli (ATCC 8739) and *Candida albicans* (ATCC 10231) using standard agar cup diffusion method [34]. The synthesized compounds were tested using ciprofloxacin and ketoconazole as antibacterial and antifungal references; respectively. Results of the antibacterial and antifungal screening are listed in Table 3.

Given the MICs in Table 3, it can be deduced that compounds **6a** and **6o** displayed potent activity against *S. aureus* compared with the reference ciprofloxacin with MICs of 1.90, 1.70 and 2.12 μg/mL, respectively. Meanwhile, ciprofloxacin derivatives **6a**, **6b**, **6i**, **6l and 6o** displayed remarkable antibacterial activity against *E. coli* compared with the reference with MICs of 2.60, 1.59, 1.95, 1.47 and 3.50 μg/mL**,** respectively. On the other hand, compounds **6e**, **6f** and **6k** exhibited weak activity against *E. coli*. Moreover, compounds **6a, 6f, 6i** and **6l** displayed a high potency against *Klebsiella pneumonia* with MIC of 1.70, 1.87, 2.98 and 1.42 μg/mL, respectively. In contrast, other compounds

Table 2
The MICs of the tested compounds 6a-c, 6f, 6h-j, 6n, 6o and the references levofloxacin (LVFX) and moxifloxacin (MFLX) against pathogenic drug-resistant and drug-susceptible strains of *M. tuberculosis.*

	6a	6b	6c	6f	6h	6i	6j	6n	6o	LVFX	MFLX
H37Rv ATCC27294	8	> 32	16	16	8	> 32	> 32	> 32	> 32	0.5	0.125
M. tuberculosis R2012-123 (pansensetive)	8	8	8	8	8	32	> 32	16	16	0.25	0.06
R-2012–59 (MDR)	4	8	8	8	4	> 32	> 32	16	> 32	0.25	≤0.03
R-2012–97 (XDR)	32	> 32	16	> 32	> 32	> 32	> 32	> 32	16	8	2
M. abscessus ATCC19977	> 32	> 32	> 32	> 32	> 32	> 32	> 32	> 32	> 32	> 32	> 32
M.chelonae ATCC35752	> 32	> 32	> 32	> 32	> 32	> 32	> 32	> 32	> 32	0.5	0.25
M.fortuitum ATCC06841	> 32	> 32	> 32	> 32	> 32	> 32	> 32	> 32	> 32	0.125	0.06

displayed moderate to weak activity against *Klebsiella pneumonia*. Compound **6o** is the only triazole derivative which showed potent activity against *ps. aeruginosa* with MICs of 1.04 μg/mL compared with the reference. Concerning the antifungal results shown in Table 3**,** it is clear that the phenyl triazole derivatives **6g** and **6l** showed considerable antifungal activity compared with the reference ketoconazole with MICs of 3.8, 6.13 and 2.60, respectively while compound **6f** exhibited weak activity compared the ketoconazole with MICs of 10.57 and 2.60, respectively. The antifungal results clearly illustrated that the presence of *p*-chlorophenyl moiety on the triazole ring seems to enhance the antifungal activity. Replacement of *p*-chlorophenyl moiety with *p*-methoxyphenyl moiety, 3,4-dimethoxyphenyl or 3,4,5-trimethoxyphenyl moiety diminishes the antifungal activity. Introduction of allyl moiety in place of the ethyl or phenyl moiety eliminates the antifungal activity.

2.3. Cleavable complex DNA gyrase assay

As previously mentioned, the antimicrobial activity of fluoroquinolones is achieved through the inhibition of type II bacterial topoisomerase enzymes (DNA gyrase subunits encoded by gyrA and gyrB), a heterotetrameric enzyme that transiently catalyzes double strand DNA breaks as it negatively supercoils DNA. Fluoroquinolones inhibit the resealing of the double strand breaks that normally follows DNA strand passage; generating persistent covalent enzyme–DNA adducts called cleaved complexes. Cleaved-complex formation in turn disrupts normal DNA replication, inducing DNA damage, and triggering cell death mechanisms. It is generally accepted that *in vitro* cleavable DNA gyrase complex assay is an excellent indictor for 4-quinolone inhibition of DNA gyrase. The ability of the newly designed derivatives to generate cleaved DNA complex was monitored by the formation of the linear DNA from a starting supercoiled plasmid using ciprofloxacin as a reference compound. The highly active antimycobacterial compounds **6c** and **6h** were selected to investigate their ability to inhibit DNA gyrase. Inhibition of DNA gyrase activity by test compounds was measured by the ability of DNA gyrase to facilitate the formation of the cleavable complex [35,36]. The results of cleavable complex DNA gyrase assay of compounds **6c** and **6h** showed their ability to poison gyrase and stimulate the formation of cleavage products; however, concentrations of these compounds to stimulate cleavage are still higher than the equivalent amount of ciprofloxacin or moxifloxacin needed to produce similar levels of cleavage Fig. 2.

2.4. Docking studies

All the synthesized ciprofloxacin derivatives **6a-o** were docked on Topoisomerase II (gyrase) (PDB: 5bs8) to predict the possible binding interactions between these compounds and the enzyme active site. Docking experiments were carried out using MOE 2014 software.

Table 4
Approximated binding free energies of tested compounds with Topoisomerase II enzyme (PDB: 5bs8) active site.

Compound	Kcal/mol	Compound	Kcal/mol
6a	−13.17	6i	−13.03
6b	−15.13	6j	−13.83
6c	−12.63	6k	−11.59
6d	−6.31	6l	−16.11
6e	−13.22	6m	−13.22
6f	−14.87	6n	−10.03
6g	−12.36	6o	−11.25
6h	−10.61	Moxifloxacin	−28.36

Target compounds have been constructed into the builder interface of MOE program, the energy was minimized until a RMSD (root mean square deviations) gradient of 0.01 Kcal/mol and RMS (Root Mean Square) distance of 0.1 Å with MMFF94X (Merck molecular force field 94x) force-field and the partial charges were automatically calculated. The optimized geometries were used for the docking study. The R value was used to inspect the quality of the PDB file. R is a measure of error between the observed intensities from the diffraction pattern and the predicted intensities that are calculated from the model. R values of 0.20 or less are taken as evidence that the model is reliable. The R value of 5bs8 was 0.196, which revealed the quality of this PDB file [37,38]. X-ray crystallographic structure of the ligand-enzyme complex were downloaded from protein data bank (www.rcsb.org); Topoisomerase II (gyrase) (PDB: 5bs8) [39]. Enzyme was prepared for docking process by automatic protein correction and adding hydrogens to the 3D structure of protein. Then, validation of the docking process was done by re-docking of the co-crystalized ligand and RMS (Root Mean Square) distance with MMFF94X force-field and the partial charges were automatically calculated and it was found of 1.59 Å. Then, the designed compounds were docked instead. Docking was carried out with the default settings of MOE-DOCK. The binding free energies from the major docked poses are listed in Table 4.

2.4.1. Binding modes of tested compounds with Topoisomerase II enzyme active site

Concerning the docking results of the reference compound, the 2D diagram showed the crucial chelation with magnesium ion (Mg 12:101) through the *C*-3 carboxylic group and *C*-4 carbonyl functionality which is mediated *via* water molecules. Such chelation is completely consistent with the mode of action of flouroquinolones [40,41]. Moreover, the reference moxifloxacin was observed to be stabilized within the active site through strong van der Waals interactions with the nucleotide bases of DNA (DG *H*11, DA *F*11, DA *E*15, DA *G*15, DT *F*10 and DT *H*10). Also, it displayed anther type of interaction *via* pi-cationic bonds with the nucleotide bases of DNA (DT *F*10 and DT *H*10). Furthermore, it forms additional Hydrogen bond with the amino acid residue Arg A

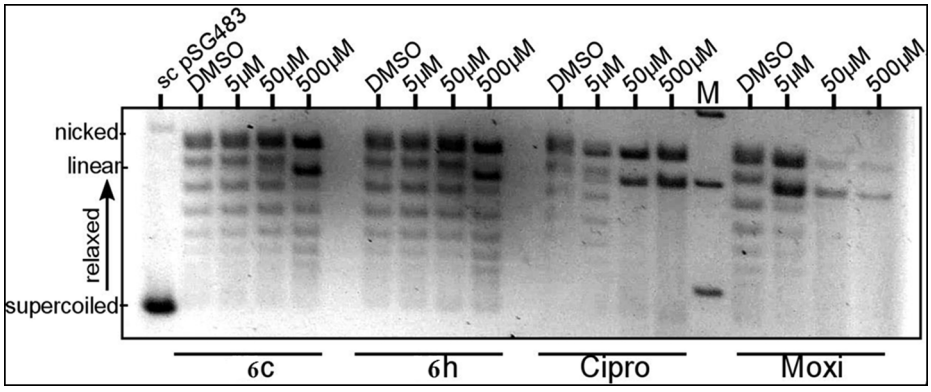

Fig. 2. DNA cleavage of MTB gyrase induced by compounds **6c** and **6h**.

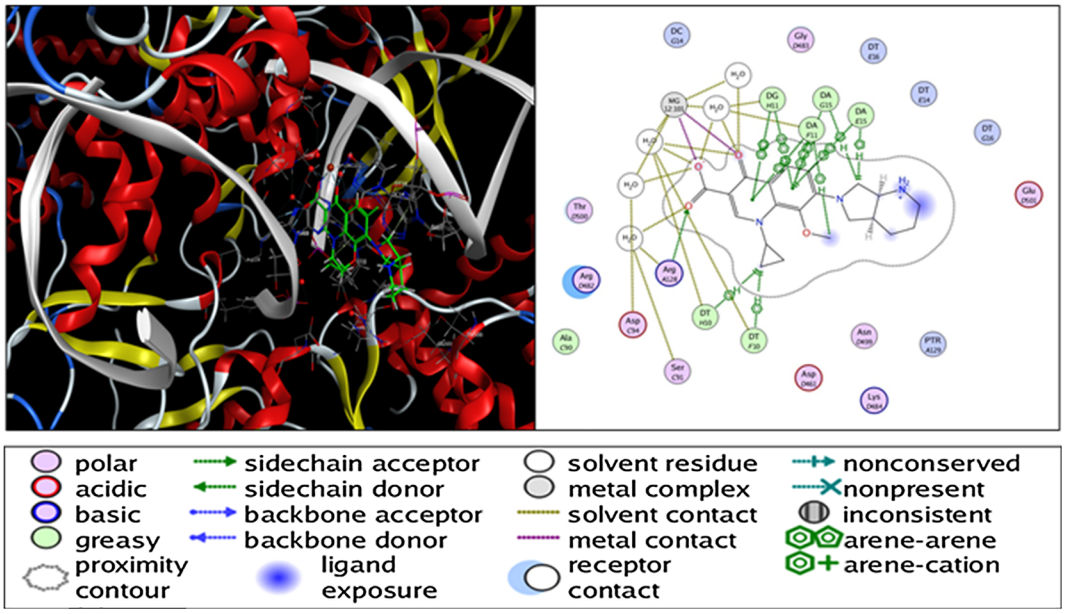

Fig. 3. 3D and 2D diagrams illustrate the binding modes of the reference **moxifloxacin** interacted with the active site of *Mycobacterium* gyrase enzyme.

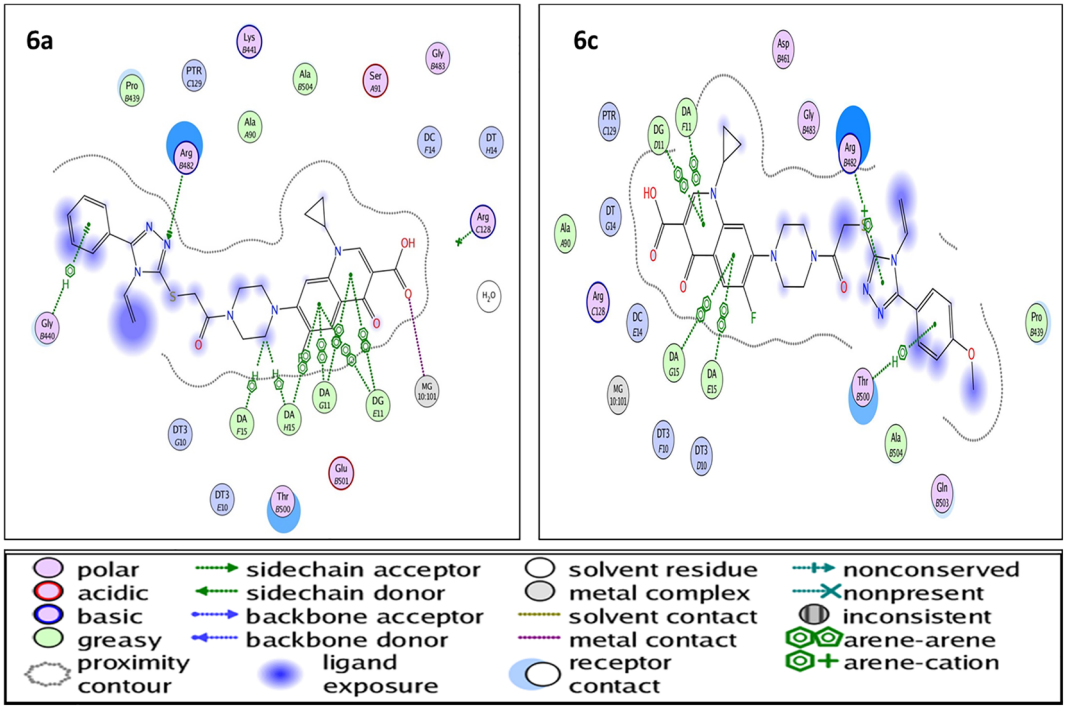

Fig. 4. 2D diagrams illustrate the binding modes of compounds **6a** and **6c** interacted with the active site of *Mycobacterium* gyrase enzyme.

128. In addition, several hydrophobic interactions observed with active site of the enzyme, Fig. 3.

Successful docking results indicated that all designed compounds were of research significance. All synthesized compounds showed binding energy scores (−6.31 to −16.11 Kcal/mol) and moderate binding interactions with the target enzyme compared with the reference moxifloxacin. Compound **6a** exhibited Van der Waals interactions with the nucleotide bases of DNA (DA *H*11 and DG *E*11). Also, it displayed anther type of interaction via pi-cationic bonds with the nucleotide bases of DNA (DA *F*15 and DA *H*15) and additional hydrogen bond interaction with the amino acid residue Arg D 182 and a pi-cationic interaction with amino acid residue Gly D 440. Moreover, the triazole derivative **6c** displayed Van der Waals interactions with the nucleotide bases of DNA (DG *D*11, DA *F*11, DA *G*15 and DA *E*15) and additional binding with amino acids residues Arg A 482 and THR B 500 Fig. 4**.** The docking studies of compound **6f** displayed comparable binding score and similar binding interactions as that of ciprofloxacin derivative **6c**. The triazole derivative **6h** displayed van der Waals interactions with the nucleotide bases of DNA (DA *F*11 and DG *F*11), Fig. 5. From the docking studies, it was found that some active compounds showed additional binding interactions with certain amino acid residues at the enzyme active site for example; compounds **6a** and **6c** displayed extra hydrogen bond interaction with the amino acid residues Arg D 182 and Arg A 482, respectively which may explain their enhanced activity against *M. smegmatis*. Furthermore, to find if there is any correlation between docking scores and their corresponding MICs,

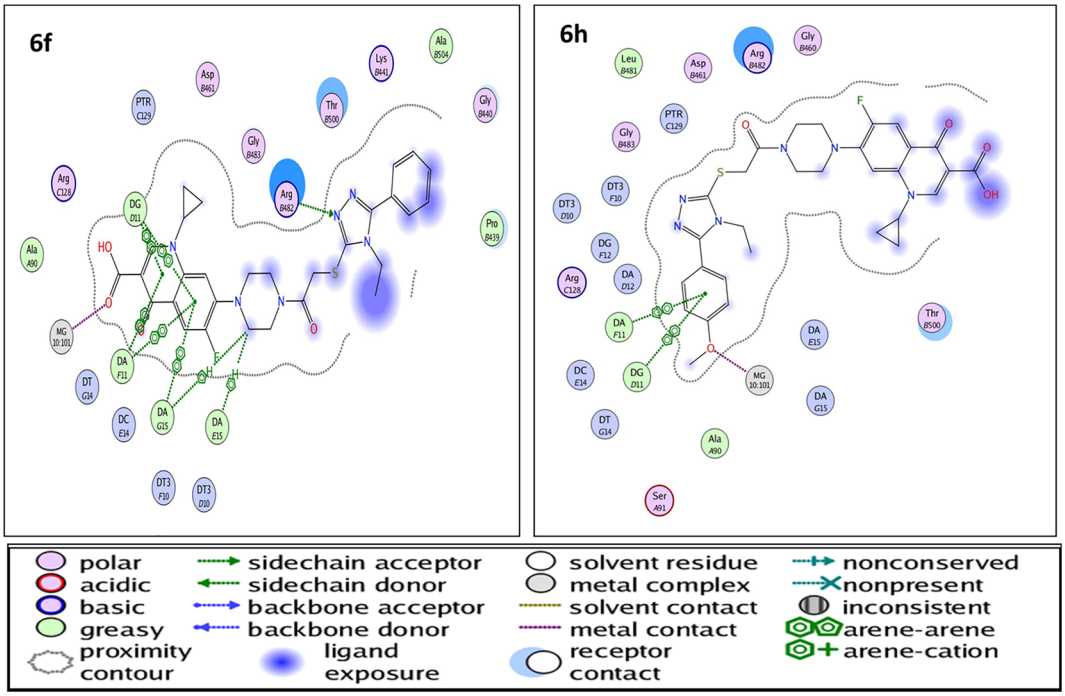

Fig. 5. 2D diagrams illustrate the binding modes of compounds **6f** and **6h** interacted with the active site of *Mycobacterium* gyrase enzyme.

Pearson correlation coefficient was calculated for docking scores and their corresponding MICs. It was found that the correlation coefficient equals (r = −0.17). A small negative value of correlation means that an increase of energy score will lead to small decrease in MICs.

3. Conclusions

New *N*-4-piperazinyl ciprofloxacin triazole hybrids were prepared and identified by different spectroscopic techniques. Biological screening results indicated that compounds **6a**, **6c** and **2h** exhibited promising antimycobacterial activity compared to the reference isoniazid against *M. smegmatis*. Also, compound **6a** displayed broad spectrum antibacterial activity against all the tested bacterial strains either Gram-positive or Gram-negative. Moreover, compounds **6g** and **6l** showed good antifungal activity compared with the reference ketoconazole. It is obvious that the unsubstituted phenyl moiety on the triazole ring improves both the antibacterial and the antimycobaterial activities as in compound **6a**. Replacement of the allyl moiety on the triazole ring by ethyl or phenyl reduces or diminishes the antimycobacterial activity as in compounds **6f, 6h, 6n** and **6o**, respectively. On the other hand, the presence of *p*-chlorophenyl moiety on the triazole ring seems to enhance the antifungal activity. Molecular docking studies illustrated that the newly designed ciprofloxacin derivatives have comparable energy scores and moderate binding interactions with the target enzyme compared with the reference moxifloxacin and this may explain the weak activity of the newly synthesized ciprofloxacin derivatives against pathogenic drug-resistant and drug-susceptible strains of *M. tuberculosis*. Compounds **6a**, **6i** and **6o** showed promising broad spectrum activity against the tested Gram-positive and Gram-negative strains. Moreover, it is obvious that the phenyl triazole derivatives **6g** and **6l** showed considerable antifungal activity compared with the reference ketoconazole with MICs of 3.8, 6.13 and 2.60, respectively. Based on the above findings, it can be concluded that, there is no specific substituent on the *N*-4-piperazine moiety of tested compounds that can determine the activity. So, the enhanced activity of some of the tested compounds may be due to improvement of the physicochemical properties and consequently enhancing permeability to microbial cells. However, *N*-4- Piperazinyl substitutions may hamper the interaction of the molecule with essential residues in the target proteins within microbial cells.

4. Experimental

4.1. Chemistry

Reactions were monitored by TLC, using Merck 9385 pre-coated aluminum plate silica gel (Kieselgel 60) 5 cm × 20 cm plates with a layer thickness of 0.2 mm. The spots were detected by exposure to UV-lamp at λ = 254 nm. Melting points were determined on Stuart electrothermal melting point apparatus and were uncorrected. IR spectra were recorded as KBr disks on a Brukar Vector 22 IR spectrophotometer. NMR spectra (400 MHz for ^{1}H, 100 MHz for ^{13}C) were observed in DMSO-d_6 on Bruker AM400 spectrometer with tetramethylsilane as the internal standard. Chemical shifts (δ) values are given in parts per million (ppm) using DMSO-d_6 as solvent and coupling constants are designated as (*J*) in Hz. Splitting patterns are designated as follows: s, singlet; d, doublet; dd, doublet of doublet; t, triplet; q, quartet; m, multiplet; brs, broad singlet. High-resolution mass spectra (HRMS) were recorded on Thermo Scientific Q Exactive™ Orbitrap mass spectrometer and reported as mass/charge (*m/z*) with percent relative abundance. The intermediates **1a-e, 2a-e, 3a-o** and **4a-o** were prepared according to reported procedures [29,42].

4.1.1. General procedure for synthesis of compounds 6a-o

An equimolar mixture of **4a-o** (0. 9 mmol) and compound **5** (0.40 g, 0.9 mmol) in acetonitrile (50 mL) and TEA (0.48 g, 0.25 mL, 1.8 mmol) was added. The reaction mixture was heated at reflux for 6–8 h. The reaction mixture was evaporated to dryness. The residue was crystallized from acetonitrile to afford the target compounds **6a-o**.

4.1.1.1. 7-(4-(2-((4-Allyl-5-phenyl-4H-1,2,4-triazol-3-yl)thio)acetyl) piperazin-1-yl)-1-cyclopropyl-6-fluoro-4-oxo-1,4-dihydroquinoline-3-carboxylic acid 6a. Yellow crystals; 0.43 g, 82.76% yield; mp: 281–282 °C; ^{1}H NMR (400 MHz, DMSO-d_6) δ 1.19–1.21 (2H, m, cyclopropyl-*H*), 1.33–1.35 (2H, m, cyclopropyl-*H*), 3.39–3.45 (4H, m, piperazinyl-*H*), 3.75–3.77 (4H, m, piperazinyl-*H*), 3.81–3.84 (1H, m,

cyclopropyl-*H*), 4.38 (2H, s, S−C$\underline{H_2}$), 4.71 (2H, d, J = 4 Hz, N−C$\underline{H_2}$−CH=CH_2), 4.88 (1H, d, J_{trans} = 16 Hz, N−CH_2−CH=C$\underline{H_2}$), 5.25 (1H, d, J_{cis} = 8 Hz, N−CH_2−CH=C$\underline{H_2}$), 5.95–6.02 (1H, m, N−CH_2−C$\underline{H}$=CH_2), 7.55–7.56 (3H, m, Ar−*H*), 7.59 (1H, d, J = 8 Hz, *H*-8), 7.63–7.65 (2H, m, Ar−*H*), 7.93 (1H, d, J = 12 Hz, *H*-5), 8.68 (1H, s, *H*-2), 15.08 (1H, brs, COO*H*); ^{13}C NMR (100 MHz, DMSO-d_6) δ 8.05, 36.30, 37.13, 41.85, 45.64, 47.01, 49.84, 107.00, 107.44, 111.68, 117.70, 119.41, 127.54, 128.64, 129.38, 130.54, 133.03, 139.68, 145.20, 148.46, 150.95, 152.50, 155.63, 166.15, 166.27, 176.89; ESI-MS (*m/z*): calcd. For $C_{30}H_{29}FN_6O_4S$ 587.18823, found 587.18903 $[M-H]^-$.

4.1.1.2. 7-(4-(2-((4-Allyl-5-(4-chlorophenyl)-4H-1,2,4-triazol-3-yl)thio) acetyl) piperazin-1-yl)-1-cyclopropyl-6-fluoro-4-oxo-1,4-dihydroquinoline-3-carboxylic acid 6b. Yellow crystals; 0.44 g, 79.94% yield; mp: 200–201 °C; ^{1}H NMR (400 MHz, DMSO-d_6) δ 1.19–1.21 (2H, m, cyclopropyl-*H*), 1.33–1.35 (2H, m, cyclopropyl-*H*), 3.39–3.45 (4H, m, piperazinyl-*H*), 3.75–3.77 (4H, m, piperazinyl-*H*), 3.81–3.83 (1H, m, cyclopropyl-*H*), 4.38 (2H, s, S−C$\underline{H_2}$), 4.71 (2H, d, J = 4 Hz, N−C$\underline{H_2}$−H=CH_2), 4.89 (1H, d, J_{trans} = 20 Hz, N−CH_2−CH=C$\underline{H_2}$), 5.25 (1H, d, J_{cis} = 8 Hz, N−CH_2−CH=C$\underline{H_2}$), 5.95–6.01(1H, m, N−CH_2−C$\underline{H}$=CH_2), 7.57–7.62 (3H, m, 2Ar−*H* and *H*-8), 7.67 (2H, d, J = 8 Hz, Ar−*H*), 7.92 (1H, d, J = 13 Hz, *H*-5), 8.67 (1H, s, *H*-2), 15.07 (1H, brs, COO*H*); ^{13}C NMR (100 MHz, DMSO-d_6) δ 8.05, 36.29, 37.15, 41.86, 45.61, 47.06, 49.53, 49.85, 106.96, 107.43, 111.66, 117.81, 119.39, 126.37, 129.53, 130.40, 132.91, 135.50, 139.65, 145.28, 148.43, 151.33, 152.14, 154.66, 166.10, 166.26, 176.86; ESI-MS (*m/z*): calcd. For $C_{30}H_{28}ClFN_6O_4S$ 621.14925, found 621.14984 $[M-H]^-$.

4.1.1.3. 7-(4-(2-((4-Allyl-5-(4-methoxyphenyl)-4H-1,2,4-triazol-3-yl)thio) acetyl)piperazin-1-yl)-1-cyclopropyl-6-fluoro-4-oxo-1,4-dihydroquinoline-3-carboxylic acid 6c. Yellow crystals; 0.42 g, 74.96% yield; mp: 276–277 °C; ^{1}H NMR (400 MHz, DMSO-d_6) δ 1.19–1.21 (2H, m, cyclopropyl-*H*), 1.33–1.34 (2H, m, cyclopropyl-*H*), 3.38–3.44 (4H, m, piperazinyl-*H*), 3.73–3.77 (4H, m, piperazinyl-*H*), 3.78–3.81 (1H, m, cyclopropyl-*H*), 3.84 (3H, s, OC$\underline{H_3}$), 4.35 (2H, s, S−C$\underline{H_2}$), 4.68 (2H, d, J = 4 Hz, N−C$\underline{H_2}$−H=CH_2), 4.87 (1H, d, J_{trans} = 20 Hz, N−CH_2−CH=C$\underline{H_2}$), 5.25 (1H, d, J_{cis} = 8 Hz, N−CH_2−CH=C$\underline{H_2}$), 5.94–6.03 (1H, m, N−CH_2−C$\underline{H}$=CH_2), 7.09 (2H, d, J = 8 Hz, Ar−*H*), 7.55–7.59 (3H, m, 2Ar−*H* and *H*-8), 7.93 (1H, d, J = 13 Hz, *H*-5), 8.67 (1H, s, *H*-2), 15.08 (1H, brs, COO*H*); ^{13}C NMR (100 MHz, DMSO-d_6) δ 8.06, 36.34, 37.27, 41.76, 45.54, 46.93, 49.50, 49.83, 55.79, 107.08, 107.23, 111.62, 114.87, 117.45, 119.58, 130.09, 133.20, 139.59, 145.23, 148.54, 150.57, 152.15, 154.63, 155.47, 161.02, 166.10, 166.38, 176.78; ESI-MS (*m/z*): calcd. For $C_{31}H_{31}FN_6O_5S$ 617.19879, found 617.19934 $[M-H]^-$.

4.1.1.4. 7-(4-(2-((4-Allyl-5-(3,4-dimethoxyphenyl)-4H-1,2,4-triazol-3-yl) thio) acetyl) piperazin-1-yl)-1-cyclopropyl-6-fluoro-4-oxo-1,4-dihydroquinoline-3-carboxylic acid 6d. Yellow crystals; 0.46 g, 80.22% yield; mp: 223–224 °C; ^{1}H NMR (400 MHz, DMSO-d_6) δ 1.20–1.22 (2H, m, cyclopropyl-*H*), 1.33–1.35 (2H, m, cyclopropyl-*H*), 3.39–3.44 (4H, m, piperazinyl-*H*), 3.74–3.77 (4H, m, piperazinyl-*H*), 3.79 (3H, s, OC$\underline{H_3}$), 3.80–3.82 (1H, m, cyclopropyl-1H), 3.84 (3H, s, OC$\underline{H_3}$), 4.35 (2H, s, S−C$\underline{H_2}$), 4.70 (2H, d, J = 4 Hz, N−C$\underline{H_2}$−H=CH_2), 4.91 (1H, d, J_{trans} = 16 Hz, N−CH_2−CH=C$\underline{H_2}$), 5.27 (1H, d, J_{cis} = 8 Hz, N−CH_2−CH=C$\underline{H_2}$), 5.97–6.04 (1H, m, N−CH_2−C$\underline{H}$=CH_2), 7.11 (1H, d, J = 8 Hz, Ar−*H*), 7.17–7.18 (2H, m, Ar−*H*), 7.59 (1H, d, J = 8 Hz, *H*-8) 7.92 (1H, d, J = 12 Hz, *H*-5), 8.67 (1H, s, *H*-2), 15.05 (1H, brs, COO*H*); ^{13}C NMR (100 MHz, DMSO-d_6) δ 8.06, 9.10, 36.34, 37.26, 41.77, 45.55, 46.22, 47.04, 49.52, 49.85, 56.04, 107.07, 107.23, 111.38, 111.95, 112.28, 117.43, 119.60, 121.31, 133.34, 139.59, 145.32, 148.52, 149.20, 150.60, 150.69, 152.14, 154.62, 155.58, 166.10, 166.36, 176.81; ESI-MS (*m/z*): calcd. For $C_{32}H_{33}N_6O_6S$ 647.20935, found 647.21008 $[M-H]^-$.

4.1.1.5. 7-(4-(2-((4-Allyl-5-(3,4,5-trimethoxyphenyl)-4H-1,2,4-triazol-3-yl) thio)acetyl) piperazin-1-yl)-1-cyclopropyl-6-fluoro-4-oxo-1,4-dihydroquinoline-3-carboxylic acid 6e. Yellow crystals; 0.43 g, 71.66% yield; mp: 297–298 °C; ^{1}H NMR (400 MHz, DMSO-d_6) δ 1.19–1.21 (2H, m, cyclopropyl-*H*), 1.31–1.34 (2H, m, cyclopropyl-*H*), 3.38–3.42 (4H, m, piperazinyl- *H*), 3.72 (3H, s, OC$\underline{H_3}$), 3.73–3.79 (4H, m, piperazinyl-*H*), 3.80 (6H, s, 2OC$\underline{H_3}$), 4.12–4.13 (1H, m, cyclopropyl-*H*), 4.41 (2H, s, S−C$\underline{H_2}$), 4.72 (2H, d, J = 4 Hz, N−C$\underline{H_2}$−H=CH_2), 4.91 (1H, d, J_{trans} = 17.2 Hz, N−CH_2−CH=C$\underline{H_2}$), 5.29 (1H, d, J_{cis} = 10.4 Hz, N−CH_2−CH=C$\underline{H_2}$), 6.02–6.09 (1H, m, NH-CH_2−C$\underline{H}$=CH_2), 6.89 (2H, s, Ar−*H*), 7.59 (1H, d, J = 7.2 Hz, *H*-8), 7.96 (1H,d, J = 13.2 Hz, $\underline{H}$-5), 8.68 (1H, s, *H*-2), 15.21 (1H, brs, COO*H*); ^{13}C NMR (100 MHz, DMSO-d_6) δ 8.07, 36.37, 37.27, 41.78, 47.16, 49.06, 49.52, 49.80, 56.49, 60.60, 106.06, 107.23, 111.39, 117.46, 119.58, 122.61, 125.23, 133.42, 134.17, 138.60, 139.63, 145.40, 148.52, 150.99, 153.56, 155.56, 166.05, 166.41, 176.81; ESI-MS (*m/z*): calcd. For $C_{33}H_{35}FN_6O_7S$ 677.21992, found 677.22070 $[M-H]^-$

4.1.1.6. 1-Cyclopropyl-7-(4-(2-((4-ethyl-5-phenyl-4H-1,2,4-triazol-3-yl) thio) acetyl) piperazin-1-yl)-6-fluoro-4-oxo-1,4-dihydroquinoline-3-carboxylic acid 6f. Yellow crystals; 0.40 g, 78.47% yield; mp: 246–247 °C; ^{1}H NMR (400 MHz, DMSO-d_6) δ 1.20–1.21 (2H, m, cyclopropyl-*H*), 1.25 (3H, t, J = 8 Hz, N−CH_2−C$\underline{H_3}$) 1.33–1.35 (2H, m, cyclopropyl-$\underline{H}$), 3.39–3.45 (4H, m, piperazinyl-*H*), 3.75–3.84 (5H, m, piperazinyl-4*H* and cyclopropyl-*H*), 4.07 (2H, q, J = 8 Hz, N−C$\underline{H_2}$−H_3) 4.40 (2H, s, S−C$\underline{H_2}$), 7.56–7.60 (4H, m, 3Ar−*H* and *H*-8), 7.64–7.66 (2H, m, Ar−*H*), 7.93 (1H, d, J = 13 Hz, *H*-5), 8.67 (1H, s, *H*-2), 15.08 (1H, brs, COO*H*); ^{13}C NMR (100 MHz, DMSO-d_6) δ 8.06, 9.11, 15.60, 36.64, 37.14, 41.78, 45.56, 49.52, 49.85, 107.23, 111.62, 119.27, 127.71, 128.81, 129.50, 130.54, 139.60, 145.33, 148.54, 150.25, 152.15, 154.63, 155.28, 166.08, 166.38, 176.83; ESI-MS (*m/z*): calcd. For $C_{29}H_{29}FN_6O_4S$ 575.18823, found 575.18860 $[M-H]^-$.

4.1.1.7. 7-(4-(2-((5-(4-Chlorophenyl)-4-ethyl-4H-1,2,4-triazol-3-yl)thio) acetyl) piperazin-1-yl)-1-cyclopropyl-6-fluoro-4-oxo-1,4-dihydroquinoline-3-carboxylic acid 6g. Yellow crystal; 0.39 g, 72.37% yield; mp: 239–240 °C; ^{1}H NMR (400 MHz, DMSO-d_6) δ 1.17–1.21 (2H, m, cyclopropyl-*H*), 1.25 (3H, t, J = 7.2 Hz, N−CH_2−C$\underline{H_3}$), 1.29–1.33 (2H, m, cyclopropyl-*H*), 3.39–3.44 (4H, m, piperazinyl-*H*), 3.72–3.80 (4H, m, piperazinyl-*H*), 3.81–3.84 (1H, m, cyclopropyl-*H*), 4.06 (2H, q, J = 7.2 Hz, N−C$\underline{H_2}$−H_3), 4.44 (2H, s, S−C$\underline{H_2}$), 7.59 (1H, d, J = 7.2 Hz, *H*-8), 7.64 (2H, d, J = 7.2 Hz, Ar−*H*), 7.69 (2H, d, J = 7.2 Hz, Ar−*H*), 7.93 (1H, d, J = 13.2 Hz, *H*-5), 8.67 (1H, s, *H*-2), 15.18 (1H, brs, COO*H*); ^{13}C NMR (100 MHz, DMSO-d_6) δ 8.07, 15.56, 36.35, 37.18, 41.79, 45.55, 49.50, 49.85, 107.25, 111.64, 119.50, 126.55, 129.63, 130.61, 135.41, 139.61, 145.23, 148.57, 150.65, 152.20, 154.29, 155.10, 166.04, 166.37, 176.85; ESI-MS (*m/z*): calcd. For $C_{29}H_{28}ClFN_6O_4S$ 609.14925, found 609.14838 $[M-H]^-$.

4.1.1.8. 1-Cyclopropyl-7-(4-(2-((4-ethyl-5-(4-methoxyphenyl)-4H-1,2,4-triazol-3-yl)thio) acetyl)piperazin-1-yl)-6-fluoro-4-oxo-1,4-dihydroquinoline-3-carboxylic acid 6h. Yellow crystals; 0.41 g, 76.59% yield; mp: 212–213 °C; ^{1}H NMR (400 MHz, DMSO-d_6) δ 1.20–1.22 (2H, m, cyclopropyl-*H*), 1.24 (3H, t, J = 8 Hz, N−CH_2−C$\underline{H_3}$), 1.33–1.34 (2H, m, cyclopropyl-*H*), 3.39–3.44 (4H, m, piperazinyl-*H*), 3.75–3.78 (4H, m, piperazinyl-*H*), 3.80–3.83 (1H, m, cyclopropyl-*H*), 3.85 (3H, s, OC$\underline{H_3}$), 4.04 (2H, q, J = 8 Hz, N−C$\underline{H_2}$−H_3) 4.37 (2H, s, S−C$\underline{H_2}$), 7.11 (2H, d, J = 8 Hz, Ar−*H*), 7.57–7.60 (3H, m, 2Ar−*H* and *H*-8), 7.93 (1H, d, J = 12 Hz, *H*-5), 8.67 (1H, s, *H*-2), 15.08 (1H, brs, COO*H*); ^{13}C NMR (100 MHz, DMSO-d_6) δ 8.05, 15.55, 36.30, 36.95, 41.85, 45.62, 49.55, 49.86, 55.84, 106.99, 107.44, 111.44, 114.95, 119.33, 120.05, 130.29, 139.66, 145.29, 148.45, 149.68, 152.15, 154.63, 155.19, 161.03, 166.72, 176.87; ESI-MS (*m/z*): calcd. For $C_{30}H_{31}FN_6O_5S$ 605.19879, found 605.19916 $[M-H]^-$.

4.1.1.9. 1-Cyclopropyl-7-(4-(2-((5-(3,4-dimethoxyphenyl)-4-ethyl-4H-1,2,4-triazol-3-yl)thio) acetyl)piperazin-1-yl)-6-fluoro-4-oxo-1,4-dihydroquinoline-3-carboxylic acid 6i. Yellow crystals; 0.45 g, 80.05% yield; mp: 229–230 °C; ^{1}H NMR (400 MHz, DMSO-d_6) δ 1.19–1.21 (2H, m, cyclopropyl-*H*), 1.22 (3H, t, J = 7.2 Hz, N−CH$_2$−C*H*$_3$), 1.31–1.33 (2H, m, cyclopropyl-*H*), 3.39–3.43 (4H, m, piperazinyl-*H*), 3.72–3.76 (4H, m, piperazinyl-*H*), 3.77–3.79 (1H, m, cyclopropyl-*H*), 3.80 (3H, s, OC*H*$_3$), 3.83 (3H, s, OC*H*$_3$), 4.05 (2H, q, J = 7.2 Hz, N−C*H*$_2$−H$_3$), 4.42 (2H, s, S−C*H*$_2$), 7.10–7.17 (3H, m, Ar−*H*), 7.58 (1H, d, J = 7.2 Hz, *H*-8), 7.94 (1H, d, J = 12.8 Hz, *H*-5), 8.67 (1H, s, *H*-2), 15.20 (1H, brs, COO*H*); ^{13}C NMR (100 MHz, DMSO-d_6) δ 5.94, 13.51, 34.23, 35.00, 39.64, 43.43, 46.94, 47.41, 47.74, 53.91, 105.10, 109.28, 110.06, 117.16, 117.23, 117.78, 119.31, 137.48, 143.21, 146.46, 147.12, 147.66, 148.46, 150.04, 152.51, 153.15, 163.98, 164.26, 174.72; ESI-MS (*m/z*): calcd. For $C_{31}H_{33}FN_6O_6S$ 635.20935, found 635.20966 [M − H]$^-$.

4.1.1.10. 1-Cyclopropyl-7-(4-(2-((4-ethyl-5-(3,4,5-trimethoxyphenyl)-4H-1,2,4-triazol-3-yl)thio)acetyl)piperazin-1-yl)-6-fluoro-4-oxo-1,4-dihydroquinoline-3-carboxylic acid 6j. Yellow crystals; 0.42 g, 71.27% yield; mp: 260–261 °C; ^{1}H NMR (400 MHz, DMSO-d_6) δ 1.21–1.22 (2H, m, cyclopropyl-*H*), 1.27 (3H, t, J = 8 Hz, N−CH$_2$−C*H*$_3$) 1.33–1.34 (2H, m, cyclopropyl-*H*), 3.40–3.46 (4H, m, piperazinyl-*H*), 3.73–3.75 (4H, m, piperazinyl-*H*), 3.76 (3H, s, OC*H*$_3$), 3.79–3.83 (1H, m, cyclopropyl-*H*), 3.84 (6H, s, 2OC*H*$_3$), 4.10 (2H, q, J = 8 Hz, N−C*H*$_2$−H$_3$) 4.39 (2H, s, S−C*H*$_2$), 6.89 (2H, s, Ar−*H*), 7.60 (1H, d, J = 8 Hz, *H*-8), 7.94 (1H, d, J = 13 Hz, *H*-5), 8.68 (1H, s, *H*-2), 15.09 (1H, brs, COO*H*); ^{13}C NMR (100 MHz, DMSO-d_6) δ 8.05, 15.59, 36.30, 36.92, 41.87, 45.64, 49.57, 49.87, 56.73, 60.64, 106.81, 106.98, 107.44, 111.45, 119.41, 123.04, 139.68, 145.29, 148.46, 149.99, 152.15, 153.69, 154.63, 155.31, 166.16, 166.25, 176.87; ESI-MS (*m/z*): calcd. For $C_{32}H_{35}FN_6O_7S$ 665.21992, found 665.22064 [M − H]$^-$.

4.1.1.11. 1-Cyclopropyl-7-(4-(2-((4,5-diphenyl-4H-1,2,4-triazol-3-yl)thio) acetyl)piperazin-1-yl)-6-fluoro-4-oxo-1,4-dihydroquinoline-3-carboxylic acid 6k. Yellow crystals; 0.39 g, 70.62% yield; mp: 271–272 °C; ^{1}H NMR (400 MHz, DMSO-d_6) δ 1.19–1.21 (2H, m, cyclopropyl-*H*), 1.33–1.35 (2H, m, cyclopropyl-*H*), 3.37–3.45 (4H, m, piperazinyl-*H*), 3.72–3.75 (4H, m, piperazinyl-*H*), 3.81–3.84 (1H, m, cyclopropyl-*H*), 4.36 (2H, s, S−C*H*$_2$), 7.33–7.38 (4H, m, Ar−*H*), 7.39–7.43 (3H, m, Ar−*H*), 7.58–7.60 (4H, m, 3Ar−*H* and *H*-8), 7.93 (1H, d, J = 12 Hz, *H*-5), 8.68 (1H, s, *H*-2), 15.08 (1H, brs, COOH); ^{13}C NMR (100 MHz, DMSO-d_6) δ 8.06, 36.30, 36.52, 41.82, 45.62, 49.47, 49.81, 106.97, 107.44, 111.44, 119.33, 127.16, 128.16, 128.35, 129.00, 130.20, 130.41, 130.51, 134.43, 139.67, 145.28, 148.45, 151.84, 152.15, 154.83, 165.96, 166.26, 176.88; ESI-MS (*m/z*): calcd. For $C_{33}H_{29}FN_6O_4S$ 623.18823, found 623.18878 [M − H]$^-$.

4.1.1.12. 7-(4-(2-((5-(4-Chlorophenyl)-4-phenyl-4H-1,2,4-triazol-3-yl)thio) acetyl)piperazin-1-yl)-1-cyclopropyl-6-fluoro-4-oxo-1,4-dihydroquinoline-3-carboxylic acid 6l. Yellow crystals; 0.45 g, 77.27% yield; mp: 283–284 °C; ^{1}H NMR (400 MHz, DMSO-d_6) δ 1.19–1.21 (2H, m, cyclopropyl-*H*), 1.32–1.34 (2H, m, cyclopropyl-*H*), 3.53–3.56 (4H, m, piperazinyl-*H*), 3.72–3.75 (4H, m, piperazinyl-*H*), 3.80–3.83 (1H, m, cyclopropyl-*H*), 4.41 (2H, s, S−C*H*$_2$), 7.36 (2H, d, J = 8.4 Hz, Ar−*H*), 7.44–7.46 (4H, m, Ar−*H*), 7.58–7.60 (4H, m, 3Ar−*H* and *H*-8), 7.94 (1H,d, J = 13.2 Hz, *H*-5), 8.68 (1H, s, *H*-2), 15.19 (1H, brs, COOH); ^{13}C NMR (100 MHz, DMSO-d_6) δ 8.07, 36.36, 36.52, 41.82, 45.56, 49.06, 106.85, 107.25, 112.01, 119.56, 126.56, 128.10, 129.25, 130.07, 130.57, 130.71, 134.12, 135.13, 138.87, 145.18, 148.45, 152.15, 154.83, 157.89, 163.10, 165.85, 176.88; ESI-MS (*m/z*): calcd. For $C_{33}H_{28}ClFN_6O_4S$ 657.14925, found 657.14984 [M − H]$^-$.

4.1.1.13. 1-Cyclopropyl-6-fluoro-7-(4-(2-((5-(4-methoxyphenyl)-4-phenyl-4H-1,2,4-triazol-3-yl)thio)acetyl)piperazin-1-yl)-4-oxo-1,4-dihydroquinoline-3-carboxylic acid 6 m. Yellow crystals; 0.45 g, 70.83% yield; mp: 270–271 °C; ^{1}H NMR (400 MHz, DMSO-d_6) δ 1.19–1.21 (2H, m, cyclopropyl-*H*), 1.32–1.33 (2H, m, cyclopropyl-*H*), 3.16–3.18 (2H, m, piperazinyl-*H*), 3.41–3.43 (2H, m, piperazinyl-*H*), 3.69–3.73 (4H, m, piperazinyl-*H),* 3.75 (3H, s, OC*H*$_3$), 3.81–3.83 (1H, m, cyclopropyl-*H*), 4.37 (2H, s, S−C*H*$_2$), 6.90 (2H, d, J = 7.2 Hz, Ar−*H*), 7.28 (2H, d, J = 7.2. Hz, Ar−*H*), 7.41–7.43 (2H, m, Ar−*H*), 7.56–7.59 (4H, m, 3Ar−*H* and *H*-8), 7.93 (1H, d, J = 13.2 Hz, *H*-5), 8.67 (1H, s, *H*-2), 15.18 (1H, brs, COOH); ^{13}C NMR (100 MHz, DMSO-d_6) δ 8.07, 36.35, 36.69, 41.73, 45.57, 49.07, 49.84, 55.70, 107.07, 107.24, 111.63, 114.53, 119.34, 128.20, 129.81, 130.48, 130.52, 134.49, 139.61, 145.22, 145.32, 148.56, 151.37, 152.15, 154.63, 160.71, 165.91, 166.38, 176.84; ESI-MS (*m/z*): calcd. For $C_{34}H_{31}FN_6O_5S$ 653.19879, found 653.19928 [M − H]$^-$.

4.1.1.14. 1-Cyclopropyl-7-(4-(2-((5-(3,4-dimethoxyphenyl)-4-phenyl-4H-1,2,4-triazol-3-yl)thio)acetyl)piperazin-1-yl)-6-fluoro-4-oxo-1,4-dihydroquinoline-3-carboxylic acid 6n. Yellow crystals; 0.39 g, 64.43% yield; mp: 276–277 °C; ^{1}H NMR (400 MHz, DMSO-d_6) δ 1.19–1.21 (2H, m, cyclopropyl-*H*), 1.33–1.35 (2H, m, cyclopropyl-*H*), 3.36–3.44 (4H, m, piperazinyl-*H*), 3.53 (3H, s, OC*H*$_3$) 3.71–3.74 (4H, m, piperazinyl-*H*), 3.75 (3H, s, OC*H*$_3$), 3.81–3.85 (1H, m, cyclopropyl-*H*), 4.33 (2H, s, S−C*H*$_2$), 6.89–6.93 (3H, m, Ar−*H*), 7.42–7.45 (2H, m, Ar−*H*), 7.58–7.61 (4H, m, 3Ar−*H* and *H*-8), 7.94 (1H, d, J = 13 Hz, *H*-5), 8.68 (1H, s, *H*-2), 15.11 (1H, brs, COOH); ESI-MS (*m/z*): calcd. For $C_{35}H_{33}FN_6O_6S$ 683.20935, found 683.20996 [M − H]$^-$.

4.1.1.15. 1-Cyclopropyl-6-fluoro-4-oxo-7-(4-(2-((4-phenyl-5-(3,4,5-trimethoxyphenyl)-4H-1,2,4-triazol-3-yl)thio)acetyl)piperazin-1-yl)-1,4-dihydroquinoline-3-carboxylic acid 6o. Yellow crystals; 0.45 g, 71.21% yield; mp 237–238 °C; ^{1}H NMR (400 MHz, DMSO-d_6) δ 1.19–1.20 (2H, m, cyclopropyl-*H*), 1.34–1.35 (2H, m, cyclopropyl-*H*), 3.37–3.44 (4H, m, piperazinyl-*H*), 3.57 (6H, s, OC*H*$_3$) 3.67 (3H, s, OC*H*$_3$), 3.72–3.75 (4H, m, piperazinyl-*H*), 3.82–3.84 (1H, m, cyclopropyl-*H*), 4.34 (2H, s, S−C*H*$_2$), 6.65 (2H, s, Ar−*H*), 7.46–7.48 (2H, m, Ar−*H*), 7.58–7.61 (4H, m, 3Ar−*H* & *H*-8), 7.93 (1H, d, J = 12 Hz, *H*-5), 8.67 (1H, s, *H*-2), 15.08 (1H, brs, COOH); ^{13}C NMR (100 MHz, DMSO-d_6) δ 8.05, 36.30, 36.41, 41.84, 45.62, 49.51, 49.81, 56.26, 60.56, 106.18, 106.95, 107.43, 111.44, 111.67, 119.32, 122.11, 128.39, 130.46, 134.69, 139.41, 139.66, 145.27, 148.45, 151.65, 152.14, 153.19, 154.49, 165.96, 166.26, 176.86; ESI-MS (*m/z*): calcd. For $C_{36}H_{35}FN_6O_7S$ 713.21992, found 713.22076 [M − H]$^-$.

4.2. Biological investigations

4.2.1. Screening of antimycobactrial activity

4.2.1.1. Materials. Middlebrook 7H9 broth, Middlebrook 7H10 agar, Middlebrook 7H11 agar, and Luria-Bertani (LB) broth were obtained from BD (Franklin Lakes, NJ or Sparks, MD). Isoniazid was purchased from Sigma (St. Louis, MO).

4.2.1.2. Methods. Mycobacterium smegmatis was grown in LB (Luria-Bertani) liquid medium with 0.05% Tween 80 for competent cell preparation at faculty of pharmaceutical sciences, Osaka University, Japan. The determination of MIC against *M. smegmatis* was performed by the established MTT method.[33] Briefly, *M. smegmatis* in the mid-logarithmic phase (1×10^4 CFU per 0.1 mL) was inoculated into each well of a 96-well plate, and then the serially diluted sample was added to each well. After 48 h incubation at 37 °C, 50 mL of MTT solution (0.5 mg/mL) was added into each well and incubation was carried out at 37 °C for an additional 6 h. The optical density (OD) at 560 nm was measured to determine MICs.

4.2.2. Screening of antibacterial activity

The antibacterial activity of compounds **6a-6b, 6e-g, 6i, 6k-6l** and **6o** and ciprofloxacin were determined according to the standard agar cup diffusion method at Department of Microbiology, Faculty of Pharmacy, Minia University, Minia, Egypt.

4.2.2.1. Microbial strains and culture conditions. Four bacterial species representing both Gram-positive and Gram-negative strains and were used to test the antibacterial activity of the new compounds. Standard strains of *Staphylococcus aureus* (ATCC 6538), *Klebsiella pneumoniae* (ATCC 10031), *Pseudomonas aeruginosa* (ATCC 10145), *Escherichia coli* (ATCC 8739) were obtained from microbiological resource center, Faculty of Agriculture, Ain Shams University, Cairo, Egypt. All isolates were maintained at −70 °C in Trypticase Soya Broth (TSB, Becton and Dickinson) with 10% glycerol. Prior to inoculation, all isolates were subcultured at 37 °C for 24 h on Trypticase Soya Agar (TSA, Becton and Dickinson) and TSB, respectively.

4.2.2.2. Determination of the minimum inhibitory concentration (MIC). From all the tested bacteria 0.5 mL of 1 × 108 CFU/mL (0.5 McFarland turbidity) were plated in sterile petri dishes, then 20 mL of Mueller Hinton Agar media (Oxoid) was added to each petri dish. The plates were rotated slowly to ensure uniform distribution of the microorganisms and then allowed to solidify on a flat surface. After solidification, four equidistant and circular wells of 10 mm diameter were carefully punched using a sterile cork bore. Two fold serial dilutions of the tested compounds using DMSO were performed. An equal volume of 100 μL of each dilution was applied separately to each well in three replicates using a micropipette. All plates were incubated at 37 °C for 24 h. The inhibition zones were measured and their average was calculated. The MIC was calculated by plotting the natural logarithm of the concentration of each dilution of the tested compounds against the square of zones of inhibition and a regression line was drawn through the points then the antilogarithm of the intercept on the logarithm of concentration axis gave the MIC value [34].

4.2.3. Screening of antifungal activity

The antifungal activity of compounds **2b, 2d, 2e, 5b, 5d, 5e, 10a, 10b, 10d, 13a, 13b, 13e, 13f, 13g, 13i, 13k, 13l and 13o** and ketoconazole were determined according to the agar cup diffusion method [34] at Department of Microbiology, Faculty of Pharmacy, Minia University, Minia, Egypt.

4.2.3.1. Fungal strains and culture conditions. *Candida albicans* was used to test the antifungal activity of the new compounds. Standard strain of *Candida albicans* (ATCC 10231) was obtained from microbiological resource center, Faculty of Agriculture, Ain Shams University, Cairo, Egypt. The isolate was maintained at −70 °C in Trypticase Soya Broth (TSB, Becton and Dickinson) with 10% glycerol. Prior to inoculation, the isolate were subcultured at 37 °C for 24 h on Trypticase Soya Agar (TSA, Becton and Dickinson) and TSB, respectively.

4.2.3.2. Determination of the minimum inhibitory concentration (MIC). From the tested *Candida albicans* 0.5 mL of 1 × 108 CFU/mL (0.5 McFarland turbidity) was plated in sterile petri dishes, then 20 mL of Sabouraud agar was added to each petri dish. The plates were rotated slowly to ensure uniform distribution of the microorganisms and then allowed to solidify on a flat surface. After solidification, four equidistant and circular wells of 10 mm diameter were carefully punched using a sterile cork bore. Two fold serial dilutions of the tested compounds using DMSO were performed. An equal volume of 100 μL of each dilution was applied separately to each well in three replicates using a micropipette. All plates were incubated at 37 °C for 24 h. The inhibition zones were measured and their average was calculated. The MIC was calculated by plotting the natural logarithm of the concentration of each dilution of the tested compounds against the square of zones of inhibition and a regression line was drawn through the points then the antilogarithm of the intercept on the logarithm of concentration axis gave the MIC value [34].

4.3. Cleavable complex DNA gyrase assay

4.3.1. Protein purification

M. tuberculosis GyrA and GyrB proteins were purified separately, as described previously (Blower, et. al. PNAS 2016). Briefly, proteins were expressed from a pET28b derivative expression plasmid, producing a TEV-cleavable hexahistadine tag at the amino-terminus. Proteins were expressed in BL21[DE3] *E. coli* cells containing the Rosetta 2 pLysS plasmid. Cells were grown to mid-log phase at 30° C and induced with 1 mM IPTG for 3 h. Cells were then harvested by centrifugation and resuspended in A800 buffer [30 mM Tris-HCl, pH 7.8; 800 mM NaCl; 10 mM imidazole, pH 8.0; 10% glycerol; 0.5 mM TCEP; 1μg/mL leupeptin; 1μg/mL pepstatin; 1 mM PMSF]. Cells were lysed by sonication and lysate was clarified by centrifugation. The soluble fraction was applied to 5 mL HisTrap HP columns and washed with 25 column volumes of A800. Captured, His_6-tagged GyrA or GyrB was eluted from the resin with B800 [30 mM Tris-HCl, pH 7.8; 800 mM NaCl; 500 mM imidazole, pH 8.0; 10% glycerol; 0.5 mM TCEP; 1μg/mL leupeptin; 1μg/mL pepstatin; 1 mM PMSF]. Proteins were dialyzed separately against C500 buffer [30 mM Tris-HCl, pH 7.8; 500 mM NaCl; 10 mM imidazole; 10% glycerol; 0.25 mM TCEP] in the presence of His6-tagged TEV protease; uncleaved His6-tagged tagged protein and TEV protease were removed by a second passage over a 5 mL HisTrap HP column. Cleaved proteins were concentrated and further purified by gel filtration over a sephacryl S-300HR column pre-equilibrated in A500 buffer [50 mM Tris pH 7.8; 500 mM KCl; 10% glycerol; 0.5 mM TCEP]. Fractions containing purified protein, as assessed by SDS-PAGE, were collected and concentrated. For storage, concentrated protein was mixed 1:1 with storage buffer [50 mM Tris 7.8; 500 mM KCl; 50% glycerol; 0.5 mM TCEP], then flash frozen as aliquots in liquid nitrogen and stored at −80 °C.

4.3.2. Cleavage assays

Fluoroquinolone compounds were resuspended in DMSO and stored at −80 °C as 2.5–10 mM stocks. Purified *M. tuberculosis* GyrA and GyrB were combined 1:1 to form the gyrase heterotetramer at a concentration of 40 μM; for assays, the holoenzyme was serially diluted in two-fold steps to a final working concentration of 1.25 μM using gyrase dilution buffer [50 mM Tris pH 7.8; 150 mM monopotassium glutamate; 5 mM MgOAc; 10% glycerol]. Cleavage assays were prepared by mixing the following on ice: 4 μL 10X supercoiled plasmid DNA (125 nM); 4 μL 10X *M. tuberculosis* gyrase heterotetramer (1.25 μM); 10 μL 4X reaction buffer [120 mM Tris pH 7.8; 38 mM MgOAc; 340 mM monopotassium glutamate; 36% glycerol; 0.4 mg/mL BSA; 4 mM TCEP]; 20 μL distilled water; 2 μL 20X fluoroquinolone compound dilutions. The final reaction conditions are as follows: 12.5 nM supercoiled DNA; 125 nM *M. tuberculosis* gyrase heterotetramer; 35 mM Tris pH 7.8; 100 mM monopotassium glutamate; 10 mM MgOAc; 10% glycerol; 100 μg/mL BSA; 1 mM TCEP; 0–500 μM fluoroquinolone compound. Cleavage reactions were conducted by incubating reactions at 37 °C in the absence of ATP for 30 min. Reactions were stopped by the addition of 2 μL 12% SDS, followed immediately by the addition of 2 μL 500 mM EDTA. Stopped reactions were then mixed with 4 μL proteinase K (3 mg/mL) and digested at 37 °C for 25 min. Stopped and digested reaction products were then mixed with 10 μL DNA loading dye, and products were resolved by running 20 μL of the reaction-dye mix on 1.5% TAE agarose gels containing either with or without 1 μg/mL ethidium bromide (EtBr). Gels were run at 35 V for 16.5 h to resolve products and post-stained by soaking for 1 h in 1 μg/mL ethidium bromide followed by 2 h destaining in water. Gels were imaged by UV transillumination using a Gel Doc EZ gel imaging system (Bio-rad) [35,36].

4.3.3. Docking study

The synthesized ciprofloxacin derivatives **6a-o** were docked on Topoisomerase II (gyrase) to predict the possible binding interactions

between these compounds and the enzyme active site. Docking experiments were carried out using MOE 2014 software. Target compounds have been constructed into the builder interface of MOE program, the energy was minimized until a RMSD (root mean square deviations) gradient of 0.01 Kcal/mol and RMS (Root Mean Square) distance of 0.1 Å with MMFF94X (Merck molecular force field 94x) force-field and the partial charges were automatically calculated. X-ray crystallographic structure of the ligand-enzyme complex were downloaded from protein data bank (www.rcsb.org); Topoisomerase II (gyrase) (PDB: 5bs8). Enzyme was prepared for docking process by automatic protein correction and adding hydrogens to the 3D structure of protein. Then, validation of the docking process was done by re-docking of the co-crystalized ligand and RMS (Root Mean Square) distance with MMFF94X force-field and the partial charges were automatically calculated and it was found of 1.59 Å. Then, the designed compounds were docked instead. Docking was carried out with the default settings of MOE-DOCK. The obtained poses were studied and the poses showed best ligand-enzyme interactions were selected and stored for energy calculations.

Conflict of interest

The authors confirm that this article content has no conflict of interest.

Acknowledgments

The authors gratefully acknowledge Dr. Safwat Rabea, (Faculty of Pharmaceutical Sciences, The University of British Columbia, Canada), for measuring the high-resolution mass spectra for the newly synthesized compounds. Also, the authors are much indebted to Dr. Ahmed S. Aboraia (Department of pharmaceutical chemistry, Faculty of Pharmacy, Assuit University) for his assist regarding docking studies. The biochemical analysis of gyrase and the synthesized inhibitors was supported by the NCI (R01-CA077373, to J.M.B.).

References

[1] G.S. Bisacchi, Origins of the Quinolone class of antibacterials: an expanded "Discovery Story": miniperspective, J. Med. Chem. 58 (2015) 4874–4882.
[2] P.C. Sharma, A. Jain, S. Jain, Fluoroquinolone antibacterials: a review on chemistry, microbiology and therapeutic prospects, Acta Pol. Pharm. 66 (2009) 587–604.
[3] P. Senthilkumar, M. Dinakaran, P. Yogeeswari, A. China, V. Nagaraja, D. Sriram, Antimycobacterial activities of novel fluoroquinolones, Biomed. Pharmacother. 63 (2009) 27–35.
[4] V.E. Anderson, N. Osheroff, Type II topoisomerases as targets for quinolone antibacterials: turning Dr. Jekyll into Mr. Hyde, Curr. Pharm. Des. 7 (2001) 337–353.
[5] V.E. Anderson, R.P. Zaniewski, F.S. Kaczmarek, T.D. Gootz, N. Osheroff, Quinolones Inhibit DNA Religation Mediated by Staphylococcus aureus topoisomerase iv changes in drug mechanism across evolutionary boundaries, J. Biol. Chem. 274 (1999) 35927–35932.
[6] J.J. Champoux, DNA topoisomerases: structure, function, and mechanism, Annu. Rev. Biochem. 70 (2001) 369–413.
[7] S.C. Ozdek, D. Miller, P.M. Flynn, H.W. Flynn, In vitro antifungal activity of the fourth generation fluoroquinolones against Candida isolates from human ocular infections, Ocul. Immunol. Inflamm. 14 (2006) 347–351.
[8] S. Srinivasan, R.M. Beema Shafreen, P. Nithyanand, P. Manisankar, S.K. Pandian, Synthesis and in vitro antimicrobial evaluation of novel fluoroquinolone derivatives, Eur. J. Med. Chem. 45 (2010) 6101–6105.
[9] L.M.M. Vieira, M.V. de Almeida, M.C.S. Lourenço, F.A.F.M. Bezerra, A.P.S. Fontes, Synthesis and antitubercular activity of palladium and platinum complexes with fluoroquinolones, Eur. J. Med. Chem. 44 (2009) 4107–4111.
[10] M. Asif, Antimicrobial and anti-tubercular activity of quinolone analogues, Sci. Int. 1 (2013) 336–349.
[11] H.H.H. Mohammed, A.A. Abd El-Hafeez, S.H. Abbas, E.M.N. Abdelhafez, G.E.-D.A. Abuo-Rahma, New antiproliferative 7-(4-(N -substituted carbamoylmethyl) piperazin-1-yl) derivatives of ciprofloxacin induce cell cycle arrest at G 2/M phase, Bioorg. Med. Chem. 24 (19) (2016) 4636–4646.
[12] R.H. Advani, H.I. Hurwitz, M.S. Gordon, S.W. Ebbinghaus, D.S. Mendelson, H.A. Wakelee, U. Hoch, J.A. Silverman, N.A. Havrilla, C.J. Berman, J.A. Fox, R.S. Allen, D.C. Adelman, Voreloxin, a first-in-class anticancer Quinolone derivative, in relapsed/refractory solid tumors: a report on two dosing schedules, Clin. Cancer Res. 16 (2010) 2167–2175.
[13] M. Abdel-Aziz, S.-E. Park, G.E.-D.A.A. Abuo-Rahma, M.A. Sayed, Y. Kwon, Novel N-4-piperazinyl-ciprofloxacin-chalcone hybrids: synthesis, physicochemical properties, anticancer and topoisomerase I and II inhibitory activity, Eur. J. Med. Chem. 69 (2013) 427–438.
[14] M.A.A. Abdullah, R.M. Abd El-Baky, H.A. Hassan, E.-S.M.N. Abdelhafez, G.E.-D.A.A. Abuo-Rahma, Fluoroquinolones as urease inhibitors: anti-proteus mirabilis activity and molecular docking studies, Am. J. Microbiol. Res. 4 (2016) 81–84.
[15] M. Daneshtalab, A. Ahmed, Nonclassical biological activities of quinolone derivatives, J. Pharm. Pharm. Sci. 15 (2011) 52–72.
[16] A. Aubry, X.-S. Pan, L.M. Fisher, V. Jarlier, E. Cambau, Mycobacterium tuberculosis DNA gyrase: interaction with quinolones and correlation with antimycobacterial drug activity, Antimicrob. Agents Chemother. 48 (2004) 1281–1288.
[17] T. Zhang, W. Shen, M. Liu, R. Zhang, M. Wang, L. Li, B. Wang, H. Guo, Y. Lu, Synthesis, antimycobacterial and antibacterial activity of fluoroquinolone derivatives containing an 3-alkoxyimino-4-(cyclopropylanimo)methylpyrrolidine moiety, Eur. J. Med. Chem. 104 (2015) 73–85.
[18] L. Zhang, K.V. Kumar, S. Rasheed, S.-L. Zhang, R.-X. Geng, C.-H. Zhou, Design, synthesis, and antibacterial evaluation of novel azolylthioether quinolones as MRSA DNA intercalators, MedChemComm. 6 (2015) 1303–1310.
[19] G.E.-D.A.A. Abuo-Rahma, H.A. Sarhan, G.F.M. Gad, Design synthesis, antibacterial activity and physicochemical parameters of novel N-4-piperazinyl derivatives of norfloxacin, Bioorg. Med. Chem. 17 (2009) 3879–3886.
[20] M.V. de Almeida, M.F. Saraiva, M.V.N. de Souza, C.F. da Costa, F.R.C. Vicente, M.C.S. Lourenço, Synthesis and antitubercular activity of lipophilic moxifloxacin and gatifloxacin derivatives, Bioorg. Med. Chem. Lett. 17 (2007) 5661–5664.
[21] G. Hu, G. Wang, N. Duan, X. Wen, T. Cao, S. Xie, W. Huang, Design, synthesis and antitumor activities of fluoroquinolone C-3 heterocycles (IV): s-triazole Schiff-Mannich bases derived from ofloxacin, Acta Pharm. Sin. B. 2 (2012) 312–317.
[22] L.L. Shen, L.A. Mitscher, P.N. Sharma, T.J. O'Donnell, D.W.T. Chu, C.S. Cooper, T. Rosen, A.G. Pernet, Mechanism of inhibition of DNA gyrase by quinolone antibacterials: a cooperative drug-DNA binding model, Biochemistry (Mosc.) 28 (1989) 3886–3894.
[23] L.L. Shen, J. Baranowski, A.G. Pernet, Mechanism of inhibition of DNA gyrase by quinolone antibacterials: specificity and cooperativity of drug binding to DNA, Biochemistry (Mosc.) 28 (1989) 3879–3885.
[24] K. Drlica, Mechanism of fluoroquinolone action, Curr. Opin. Microbiol. 2 (1999) 504–508.
[25] A. Foroumadi, S. Emami, S. Rajabalian, M. Badinloo, N. Mohammadhosseini, A. Shafiee, N-Substituted piperazinyl quinolones as potential cytotoxic agents: Structure–activity relationships study, Biomed. Pharmacother. 63 (2009) 216–220.
[26] L.-S. Feng, M.-L. Liu, B. Wang, Y. Chai, X.-Q. Hao, S. Meng, H.-Y. Guo, Synthesis and in vitro antimycobacterial activity of balofloxacin ethylene isatin derivatives, Eur. J. Med. Chem. 45 (2010) 3407–3412.
[27] S.-F. Cui, Y. Ren, S.-L. Zhang, X.-M. Peng, G.L.V. Damu, R.-X. Geng, C.-H. Zhou, Synthesis and biological evaluation of a class of quinolone triazoles as potential antimicrobial agents and their interactions with calf thymus DNA, Bioorg. Med. Chem. Lett. 23 (2013) 3267–3272.
[28] H.A.A. Ezelarab, S.H. Abbas, H.A. Hassan, G.E.-D.A.A. Abuo-Rahma, Recent updates of fluoroquinolones as antibacterial agents, Arch. Pharm. Chem. Life Sci. 351 (9) (2018) 1800141.
[29] J.R. Maxwell, D.A. Wasdahl, A.C. Wolfson, V.I. Stenberg, Synthesis of 5-aryl-2H-tetrazoles, 5-aryl-2H-tetrazole-2-acetic acids, and [(4-phenyl-5-aryl-4H-1,2,4-triazol-3-yl)thio]acetic acids as possible superoxide scavengers and antiinflammatory agents, J. Med. Chem. 27 (1984) 1565–1570.
[30] R. Akhtar, M. Yousaf, S.A.R. Naqvi, M. Irfan, A.F. Zahoor, A.I. Hussain, S.A.S. Chatha, Synthesis of ciprofloxacin-based compounds: A review, Synth. Commun. 46 (2016) 1849–1879.
[31] G.E.-D.A.A. Abuo-Rahma, M. Abdel-Aziz, E.A.M. Beshr, T.F.S. Ali, 1,2,4-Triazole/oxime hybrids as new strategy for nitric oxide donors: Synthesis, anti-inflammatory, ulceroginicity and antiproliferative activities, Eur. J. Med. Chem. 71 (2014) 185–198.
[32] M.E. Shoman, M. Abdel-Aziz, O.M. Aly, H.H. Farag, M.A. Morsy, Synthesis and investigation of anti-inflammatory activity and gastric ulcerogenicity of novel nitric oxide-donating pyrazoline derivatives, Eur. J. Med. Chem. 44 (2009) 3068–3076.
[33] G. Abate, A. Aseffa, A. Selassie, S. Goshu, B. Fekade, D. WoldeMeskal, H. Miörner, Direct colorimetric assay for rapid detection of rifampin-resistant Mycobacterium tuberculosis, J. Clin. Microbiol. 42 (2004) 871–873.
[34] B. Bonev, J. Hooper, J. Parisot, Principles of assessing bacterial susceptibility to antibiotics using the agar diffusion method, J. Antimicrob. Chemother. 61 (2008) 1295–1301.
[35] J.F. Barrett, J.I. Bernstein, H.M. Krause, J.J. Hilliard, K.A. Ohemeng, Testing potential gyrase inhibitors of bacterial DNA gyrase: a comparison of the supercoiling inhibition assay and "cleavable complex" assay, Anal. Biochem. 214 (1993) 313–317.
[36] A. Mustaev, M. Malik, X. Zhao, N. Kurepina, G. Luan, L.M. Oppegard, H. Hiasa, K.R. Marks, R.J. Kerns, J.M. Berger, K. Drlica, Fluoroquinolone-gyrase-DNA complexes: two modes of drug binding, J. Biol. Chem. 289 (2014) 12300–12312.
[37] M. Harel, I. Schalk, L. Ehret-Sabatier, F. Bouet, M. Goeldner, C. Hirth, P.H. Axelsen, I. Silman, J.L. Sussman, Quaternary ligand binding to aromatic residues in the active-site gorge of acetylcholinesterase, Proc. Natl. Acad. Sci. U.S.A. 90 (1993) 9031–9035.
[38] S. Gharaghani, T. Khayamian, M. Ebrahimi, Molecular dynamics simulation study and molecular docking descriptors in structure-based QSAR on acetylcholinesterase (AChE) inhibitors, SAR QSAR Environ. Res. 24 (2013) 773–794.

[39] T.R. Blower, B.H. Williamson, R.J. Kerns, J.M. Berger, Crystal structure and stability of gyrase-fluoroquinolone cleaved complexes from Mycobacterium tuberculosis, Proc. Natl. Acad. Sci. U. S. A. 113 (2016) 1706–1713.
[40] K.J. Aldred, S.A. McPherson, C.L. Turnbough, R.J. Kerns, N. Osheroff, Topoisomerase IV-quinolone interactions are mediated through a water-metal ion bridge: mechanistic basis of quinolone resistance, Nucleic Acids Res. 41 (2013) 4628–4639.
[41] C. Sissi, B. Cheng, V. Lombardo, Y.-C. Tse-Dinh, M. Palumbo, Metal ion and inter-domain interactions as functional networks in E. coli topoisomerase I, Gene 524 (2013) 253–260.
[42] M. Abdel-Aziz, G.E.-D.A.A. Abuo-Rahma, E.A.M. Beshr, T.F.S. Ali, New nitric oxide donating 1,2,4-triazole/oxime hybrids: Synthesis, investigation of anti-in-flammatory, ulceroginic liability and antiproliferative activities, Bioorg. Med. Chem. 21 (2013) 3839–3849.